https://doi.org/10.5194/npg-2019-36
Preprint. Discussion started: 2 July 2019

Nonlinear Processes in Geophysics
Discussions
Open Access

BP Neural Network and improved Particle Swarm Optimization for Transient Electromagnetic Inversion

Huaiqing Zhang*, Ruiyou Li, Nian Yu, Ruiheng Li, Qiong Zhuang

The State Key Laboratory of Transmission Equipment and System Safety and Electrical New Technology, Chongqing University, Chongqing, 400044, China

zhanghuaiqing@cqu.edu.cn (Huaiqing Zhang); 1378546842@qq.com (Ruiyou Li); 61408155@qq.com (Nian Yu); 392361773@qq.com (Ruiheng Li) ;779695034@qq.com (Qiong Zhuang)

**Correspondence to*: zhanghuaiqing@cqu.edu.cn

Abstract. As one of the most active nonlinear inversion methods in transient electromagnetic (TEM) inversion, the back propagation (BP) neural network has high efficiency because the complicated forward model calculation is unnecessary in iteration. The global optimization ability of the particle swarm optimization (PSO) is adopted for amending BP's sensitivity on initial parameters, which avoids it falling into local optimum. A chaotic oscillation inertia weight PSO (COPSO) is proposed in accelerating convergence. The COPSO-BP algorithm performance is validated by two typical testing functions and then by two geoelectric models inversion. The results show that the COPSO-BP method has better accuracy, stability and relative less training times. The proposed algorithm has a higher fitting degree for the data inversion, and it is feasible in geophysical inverse applications.

Keywords： transient electromagnetic inversion; BP neural network; particle swarm optimization; chaotic oscillation

1 Introduction

Transient electromagnetic (TEM) method applies the secondary receiving voltage induced by the rapid switching off pulse current, and then deduces the geoelectric structure parameters. The later is a typical TEM inversion issues with nonlinear feature. The linear inversion method was simple and widely used through linearization process, yet it is extremely dependent on initial parameters selection and resulting in poor inversion accuracy. Hence, the nonlinear inversion methods attract more geophysicists attention in recent years.

The artificial neural network(ANN) is one of the most active nonlinear inversion methods, it has very high computation efficiency because the complicated forward model calculation is unnecessary in iteration. All the geoelectric parameters and the forward model relations are

Conflicts of Interests

The authors declare that they have no conflict of interest.

implied in the weight and threshold parameters of ANN. And it is different from the non-linear Monte Carlo method with global space search solution (He et al., 2018; Jha et al., 2008; Pekşen et al., 2014; Sharma, 2012; Tran and Hiltunen, 2012). Srinivas et al. (2012) compared the inversion performance of BP, radial basis function(RBF) and generalized regression neural network (GRNN) in vertical electrical sounding data, then established a 1-D inversion model with BP and finally realized the parameters inversion. Maiti et al. (2012) proposed a Bayesian neural network training method in 1-D electrical sounding. Jiang et al. (2018) improved the training method for kernel principal component wavelet neural network and achieved the resistivity imaging. Jiang et al. (2016a) gave a learning algorithm based on information criterion (IC) and particle swarm optimization for RBF network which improves the global search ability. Johnson (2017) utilized neural network method to invert multi-layer georesistivity sounding. Jiang et al. (2016b) presented a pruning Bayesian neural network (PBNN) method for resistivity imaging and solved the instability, local minimization problems. Raj et al. (2014) solved non-linear apparent resistivity inversion problems with ANN. The ANN has been widely applied in electric prospecting data interpretation for its powerful fitting ability. However, the neural network method is sensitive to initial parameter settings and falls easily into local minimum. Lots improved methods were proposed for balancing the convergence rate and inversion quality. Zhang and Liu (2011) proposed ant colony optimization for ANN and applied in high density resistivity, acquired smaller inversion errors and higher determinant coefficients. Dai et al. (2014) suggested a differential evolution (DE) for BP which enhanced the global search ability. Marina et al. (2014) introduced the genetic algorithm for ANN.

The Particle swarm optimization (PSO) has simple structure, fast convergence rate, high accuracy and global optimization ability. Fernndez et al. (2010) successfully introduced the PSO in 1-D resistivity inversion. Godio and Santilano (2018) applied it in geophysical inversion and deduced a depth resistivity earth model. Since the PSO's global searching performance, the BP's initial weights and thresholds can be trained by PSO and then the BP's global optimization ability can be improved. Comparing to the standard PSO (SPSO), a chaotic oscillation inertia weight PSO (COPSO) which can accelerate the convergence rate in the early stage was proposed naturally.

The paper structure is as following: the principle of PSO algorithm with different inertia weights schemes, the BP neural network and the proposed COPSO-BP algorithm are given in section 2. Then, the COPSO-BP algorithm performance is validated by two typical testing functions in section 3. And in later section, inversion simulations of a three-layer and five-layer geoelectric models are carried out, the hidden layer neuron numbers determining method is put forward and algorithms performance is compared.

2 Principle of COPSO-BP Algorithms

2.1 Chaotic Oscillation PSO algorithm

https://doi.org/10.5194/npg-2019-36
Preprint. Discussion started: 2 July 2019

For N-dimensional optimization problem, supposing the position (resistivity and thickness for layered model parameters inversion) and velocity(update speed) of the i-th particle (global search group number) at time t are $x_i= (x_{i1}, x_{i2},\cdots, x_{iN})$ and $v_i= (v_{i1}, v_{i2},\cdots, v_{iN})$ respectively. Then, at time t+1 ,they can be calculated by the iterations as

$$v_{id}^{t+1} = \omega \cdot v_{id}^{t} + c_1 r_1 (p_{id}^{t} - x_{id}^{t}) + c_2 r_2 (p_{gd}^{t} - x_{id}^{t}) \tag{1}$$

$$x_{id}^{t+1} = x_{id}^{t} + v_{id}^{t+1} \tag{2}$$

where r_1,r_2 are random value evenly distributed in the interval (0,1), c_1,c_2 are learning factors (usually equal to 2). And p_{id}, p_{gd} means the individual and global maximum.

The inertia weight parameter ω affects the algorithm performance seriously. A fixed weight always was used in the early time, and then various dynamic weights were proposed. Shi et al. (2010) have summarized several methods as

$$\omega_1(t) = \omega_{\mathrm{s}} - (\omega_{\mathrm{s}} - \omega_{\mathrm{e}})\, t/T_{\max} \tag{3}$$

$$\omega_2(t) = \omega_{\mathrm{s}} - (\omega_{\mathrm{s}} - \omega_{\mathrm{e}})(t/T_{\max})^2 \tag{4}$$

$$\omega_3(t) = \omega_{\mathrm{s}} - (\omega_{\mathrm{s}} - \omega_{\mathrm{e}})\left[2t/T_{\max} - (t/T_{\max})^2\right] \tag{5}$$

Where ω_{s} and ω_{e} are the start and end weight. The t, $T_{\max}$ are the current and maximum iteration. The above weights are of smooth and monotonically decreasing. In this paper, we proposed a decreasing oscillation weights scheme which was based on chaotic logistic equation. Its specific calculation formula as

$$x_{t+1} = \mu x_t \left(1 - x_t\right) \qquad t = 0,1,2,\cdots,n \tag{6}$$

$$\omega_{\mathrm{c}}\left(t\right) = \omega_{\mathrm{e}} + \left(\omega_{\mathrm{s}} - \omega_{\mathrm{e}}\right)\left(0.99^t \cdot x_t\right) \tag{7}$$

where μ is the control parameter. A complete chaos state is established for $x\in(0,1)$ and μ = 4, an inertia weight is then obtained from Eq.(7). Numerical experiments were carried out correspondingly and showed that the initial value of x_0 has little effect on inertia weight ω. The inertia weights comparison was shown in Fig.1 where $x_0 = 0.234$ and $\mu = 4$ for chaotic oscillation.

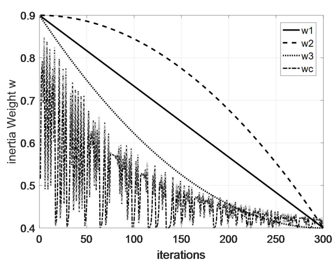

Fig. 1 Inertial weight curves comparison

https://doi.org/10.5194/npg-2019-36
Preprint. Discussion started: 2 July 2019

Nonlinear Processes in Geophysics
Discussions
Open Access

2.2 BP Neural Network

BP neural network is multi-layer feed forward structure, and a typical three-layer network is shown in Fig. 2 (Yong et al., 2009).

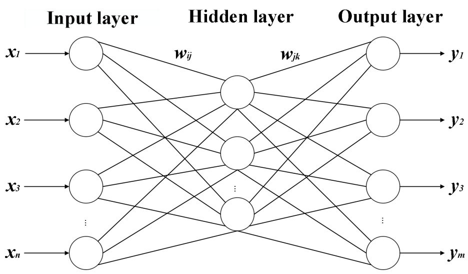

Fig. 2 Three-layer BP neural network structure

where $x_1, x_2, \ldots, x_n$ are the input value, $y_1, y_2, \ldots, y_m$ are the predicted output, w_{ij}, w_{jk} are the network weights. The threshold parameter α is defined in hidden layer with its output

$$H_j = f\left(\sum_{i=1}^{n} w_{ij} x_i - \alpha_j\right) \qquad j = 1, 2, \cdots, l \tag{8}$$

where l is the hidden layer nodes numbers, f is the activation function with different expressions, and the most widely used is sigmoid type function. The predicted output for the k-th unit is calculated by

$$O_k = \sum_{j=1}^{l} H_j w_{jk} - b_k \tag{9}$$

And parameter b means the output threshold. Then the prediction error can be determined based on predicted output O_k and the expected output T_k as $e_k = (T_k - O_k) O_k (1 - O_k)$. The updating formula for weights and thresholds are as following

$$\begin{cases} w_{ij} = w_{ij} + \eta H_j (1 - H_j) x_i \sum_{k=1}^{m} w_{jk} e_k \\ w_{jk} = w_{jk} + \eta H_j e_k \\ \alpha_j = \alpha_j + \eta H_j (1 - H_j) \sum_{k=1}^{m} w_{jk} e_k \\ b_k = b_k + e_k \end{cases} \tag{10}$$

where $i = 1, 2, \ldots, n$; $j = 1, 2, \ldots, l$; $k = 1, 2, \ldots, m$; and η is the learning rate.

2.3 BP Neural Network with COPSO algorithm

The initial parameters are chosen randomly, which affects the convergence rate, learning efficiency and perhaps falling into local minimum. The Chaotic Oscillation PSO (COPSO) has a much better global optimization capability, therefore, we proposed the COPSO algorithm for BP parameters' training. The COPSO-BP pseudo-codes were briefly described as following:

https://doi.org/10.5194/npg-2019-36
Preprint. Discussion started: 2 July 2019

Nonlinear Processes in Geophysics
Discussions
Open Access
EGU

Table.1 Pseudo-codes of COPSO-BP algorithm

BP network structure definition (neuron numbers n,l,m, and *activation function*)
COPSO initialization for BP (weights, threshold as X. PSO parameters as $V_{\min},V_{\max},\omega_c,c_1,c_2$, size M, $T_{\max}$)
Initializing BP with X_i ($i=1,2,\ldots,M$) and *evaluating fitness* by Eq.(11) for each individual
Setting the $\boldsymbol{p_{id}}$ and $\boldsymbol{p_{gd}}$
While $iter< T_{\max}$ **do**
updating inertia weight by Eq.(7)
for $i=1:M$ (all particles) **do**
updating velocity V_i by Eq.(1)
updating particle position X_i by Eq.(2)
Initializing BP with new X_i and *calculating fitness* by Eq.(11)
if X_i is better than $\boldsymbol{p_{id}}$
Set X_i is to be $\boldsymbol{p_{id}}$
End if
if X_i is better than $\boldsymbol{p_{gd}}$
Set X_i is to be $\boldsymbol{p_{gd}}$
End if
End for *i*
$iter = iter+1$
End While
Initializing BP with $\boldsymbol{p_{gd}}$
Inputting and obtaining the predicted output

The formula for calculating the i-th particle fitness is defined as

$$f_i = \frac{1}{S}\sum_{s=1}^{S}\sum_{j=1}^{m}\left(Y_{sj}-\hat{Y}_{sj}\right)^2 \tag{11}$$

where S is the number of training set samples, m is the output neurons number, Y_{sj} is the j-th reference output of the s-th sample, and $\hat{Y}_{sj}$ is the corresponding predict output.

3 Algorithm Testing

In order to investigate the COPSO-BP performance and reliability, two typical testing functions were adopted and simulations were performed in MATLAB.

(1) *Rosenbrock* function：

$$f_1 = 100\times\left(x_1^2-x_2\right)^2+\left(1-x_1\right)^2, x_i\in\left[-10,10\right], i=1,2 \tag{12}$$

(2) *Bohachevsky* function：

$$f_2\left(x\right) = x_1^2+x_2^3-x_1x_2x_3+x_3-\sin\left(x_2^2\right)-\cos\left(x_1x_3^2\right), x_i\in\left[-2\pi,2\pi\right], i=1,2,3 \tag{13}$$

https://doi.org/10.5194/npg-2019-36
Preprint. Discussion started: 2 July 2019

Nonlinear Processes in Geophysics
Discussions

The standard PSO-BP (SPSO-BP) with fixed inertia weight, the COPSO-BP were carried out respectively. The three-layer BP of *n*-*s*-1 structure is constructed with different hidden nodes. The PSO parameters are population size M = 60, learning factors $c_1 = c_2 = 2.0$, the maximum iteration $T_{\max} = 30$, inertia weight $\omega_s = 0.9$, $\omega_e = 0.4$, $x_0 = 0.234$ and $\mu = 4$ for chaotic parameters, the search dimension $D = n\times s+s\times 1+s+1$ which includes all the neuron weights and thresholds. For BP network, 150 training samples and 50 testing samples were randomly produced within the variable range. The training error is defined as

$$E = \frac{1}{S}\sum_{s}^{S}\left(T_s - O_s\right)^2 \tag{14}$$

where S is the training samples number, T_k, O_k are the expected and predicted output for training sample s respectively. The network structures with minimum training errors for *Rosenbrock* and *Bohachevsky* functions are 2-7-1 and 3-6-1 respectively. The simulation performs 20 times for each testing function with SPSO-BP and COPSO-BP algorithms. The numerical result was shown in Table.2. One of the evolutionary training error curves were shown in Fig.3, and the fitting curves of COPSO-BP algorithm were shown in Fig.4.

Table.2 Comparison of SPSO-BP and COPSO-BP algorithm for testing functions

Testing functions	SPSO-BP		COPSO-BP	
	Average value	Optimal value	Average value	Optimal value
Rosenbrock	2.375e-3	2.300e-5	5.226e-3	2.410e-06
Bohachevsky	0.225	1.024e-3	0.193	3.360e-4

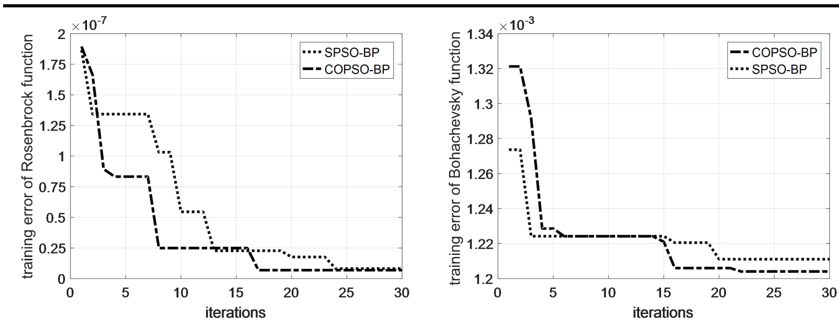

Fig. 3 Training error curves of SPSO-BP and COPSO-BP algorithms

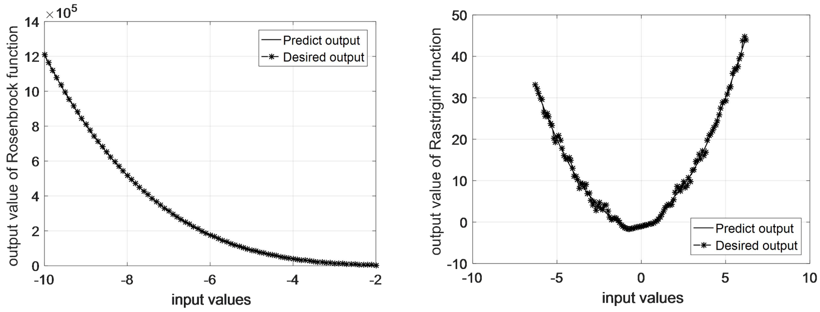

Fig. 4 Fitting curves of COPSO-BP algorithm

It can be seen in Table.2 that both the SPSO-BP and COPSO-BP algorithms can acquire a relative high accuracy for testing functions, the COPSO-BP is a litter better than SPSO-BP. However, the COPSO-BP has better convergence rate and optimization efficiency in the early stage in Fig.3. Therefore, the SPSO-BP and COPSO-BP algorithms have strong learning ability, good stability and generalization ability, which will be suitable for TEM inversion.

4 Layered model and parameter analysis

4.1 Forward Model

According to Kaufman's derivation (1983), the frequency response of central loop source for the layered model takes the following Hankel transform

$$H_z(\rho,\omega) = Ia\int_0^{\infty} \frac{m^2}{m + m_1 / R_1^*} J_1(m\rho)\,\mathrm{d}m \tag{15}$$

where a is the radius of transmitting coil, I is the excitation current, ρ is the center distance between the transmitting coil and the receiving coil, $J_1(m\rho)$ is the first-order Bessel function, m is integral variable, $m_1 = (m^2 - k_1^2)^{1/2}$, k_1 is the conduction current, σ_1 is the conductivity, $k_1 = -i\omega\mu\sigma_1$, and R_1^* is the first layer apparent resistivity conversion function which can be obtained by the following recurrence formula

$$\begin{cases} R_n^* = 1 \\ R_j^* = \dfrac{m_j R_{j+1}^* + m_{j+1}\mathrm{th}\left(m_j h_j\right)}{m_{j+1} + m_j R_{j+1}^* \mathrm{th}\left(m_j h_j\right)} \end{cases} \tag{16}$$

There is no analytical solution for the time-domain response for layered model, it can only be solved by numerical calculation. The Hankel transform in formula (15) can be calculated by fast algorithm as filter method, and then time response can be obtained using the Gaver-Stehfest transform as follows:

$$H_z(\rho,t) = \frac{\ln 2}{t}\sum_{n=1}^{\mathrm{N}} K_n H_z(\rho, s_n) \tag{17}$$

where $s_n = (\ln 2/t) \times n$, K_n is the coefficient, N is determined by the computer bits, generally N=12.

The ramp excitation current of TEM is

https://doi.org/10.5194/npg-2019-36
Preprint. Discussion started: 2 July 2019

$$I(t)=\begin{cases}0, & t<0\\ t/T_1, & 0\le t<T_1\\ 1, & T_1<t\end{cases} \tag{18}$$

where T_1 is the turn-off time, and the Laplace transform is

$$I(s)=\frac{1}{T_1 s^2}-\frac{1}{T_1 s^2}e^{-T_1 s}=\frac{1}{T_1 s^2}(1-e^{-T_1 s}) \tag{19}$$

Therefore, for a specific layered model, the apparent resistivity conversion function R_1^* is firstly calculated by recurrence formula (16) based on geoelectric structure parameters. And then the frequency response at fixed point $H_z(\omega)$ is calculated by Hankel transform as formula (15). For ramp excitation, the Laplace transform of $H_z(s)$ should multiplied by $I(s)$. Finally, the time response $H_z(t)$ is obtained by Gaver-Stehfest transform as formula (17). So the $H_z(t)$ is obtained by a Gaver-Stehfest transform, a Hankel transform and a recurrence calculation, and it is somewhat heavy computational consuming.

However, the vertical magnetic field $H_z(t)$ is the actual observed signal in transient electromagnetic method in engineering applications. It is the inversion input and output is geoelectric structure parameters. A method which can avoid the complicated forward model calculation is of great importance in algorithm efficiency.

4.2 BP network design and COPSO algorithm

For BP structure, the output nodes are determined by the number of inversion geoelectric parameters, the input nodes are determined by the samples number of $H_z(t)$, the hidden nodes varies according to approximation performance. As a three-layer or five-layer geoelectric model, its geoelectric parameters are 5 (three resistivity and two thickness parameters) or 9 (five resistivity and four thickness parameters), the output nodes are 5 or 9 correspondingly. The characteristic samplings of $H_z(t)$ are chosen as 10 or 20, which are determined by the model's complexity, more layers mean mores sampling points needed. The 10 samplings were selected in this paper hence with 10 input nodes. While for the hidden layer neuron, its number is related to the weights and threshold parameters amount directly and affects the BP performance greatly. An appropriate hidden nodes number is necessary and a determination coefficient R^2 is defined for evaluating as

$$R^2=\frac{\left(n\sum_{i=1}^{n}Y_i\hat{Y}_i-\sum_{i=1}^{n}Y_i\sum_{i=1}^{n}\hat{Y}_i\right)^2}{\left(n\sum_{i=1}^{n}\hat{Y}_i^2-\left(\sum_{i=1}^{n}\hat{Y}_i\right)^2\right)\left(n\sum_{i=1}^{n}Y_i^2-\left(\sum_{i=1}^{n}Y_i\right)^2\right)} \tag{20}$$

where Y_i is the reference value, $\hat{Y}_i$ is the predicted value for i-th training data, n is the training data number. A larger determination coefficient means a better approximation performance. The

https://doi.org/10.5194/npg-2019-36
Preprint. Discussion started: 2 July 2019

simulations on hidden nodes effect were carried out for a three-layer and five-layer geoelectric models. The BP structure is 10-*s*-5 and 10-*s*-9, its transfer, training and learning functions are 'Log sigmodial', 'Levenberg-Marquardt' and 'Gradient descent momentum' respectively. The average, minimum and maximum value of R^2 were obtained after running 20 times for each simulation. The R^2 curves were shown in Fig.5.

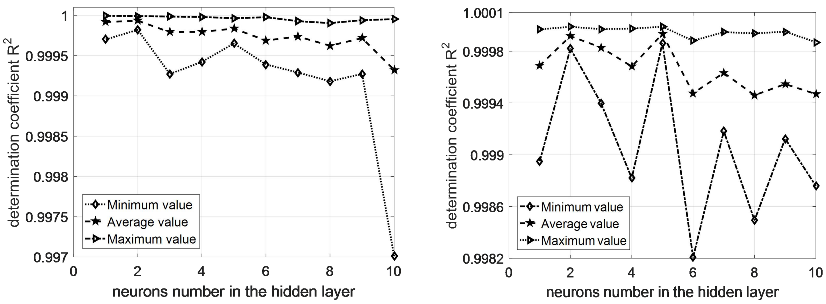

（a）Three-layer geoelectric model　　（b）Five-layer geoelectric model

Fig. 5 Influence of hidden layer nodes on R^2 for different geoelectric model

It can be seen that the optimal neural network structures were 10-2-5 and 10-5-9 for three and five-layer models based on the maximum R^2. Then, the PSO-BP algorithms with different inertia weight were implemented and compared for three-layer model. The BP structure was chosen as 10-2-5, four types of inertia weight as Eq. (3~7) in PSO were compared in Table.3.

Table.3 Comparison of different inertia weights in PSO algorithms

inertia weight	iteration number	minimum fitness	average fitness	convergence time(s)
ω_1	9	1.3914e-3	1.3982e-3	65.21
ω_2	29	1.4406e-3	1.4418e-3	204.97
ω_3	25	1.4168e-3	1.4224e-3	189.17
ω_c	6	1.3846e-3	1.3925e-3	44.34

The simulation was implemented on Core (TM) i5-7500 with 8GB memory. It is obviously found in Table.3 that the COPSO algorithm has much faster convergence rate, less iteration number and time consuming.

4.3 Layered model inversion

A 3-layered and 5-layered geoelectric models were investigated. In order to simulate actual TEM applications, the ramp turn-off is taken into account. Considering the probability distribution characteristic of above algorithms, the average of 20 simulation results is chosen. The BP, SPSO-BP, COPSO-BP algorithms and non-linear programming genetic algorithm (NPGA) (Li et al., 2017) were compared.

(1) ***3-layered H type model***

The central loop TEM parameters are set as following, transmitting coil radius a = 100 m, ramp

https://doi.org/10.5194/npg-2019-36
Preprint. Discussion started: 2 July 2019

Nonlinear Processes in Geophysics Discussions
Open Access
EGU

emission current is 100 A, turn-off time is 1 μs. In the geoelectric model, the resistivity ρ_1 = 100 Ω·m, ρ_2 = 10 Ω·m, ρ_3 = 100 Ω·m and thickness h_1 = 100 m, h_2 = 200 m.

The BP training samples which is a series of $H_z(t)$ for different geoelectric parameters were generated by TEM forward model. The resistivity ranges were $\rho_1 \in (50,150)$, $\rho_2 \in (5,15)$, $\rho_3 \in (50,150)$, the thickness range were $h_1 \in (50,150)$, $h_2 \in (100,300)$, and choosing 1000 random groups. The resistivity and thickness distributions of ρ_1 and h_1 were shown in Fig.6.

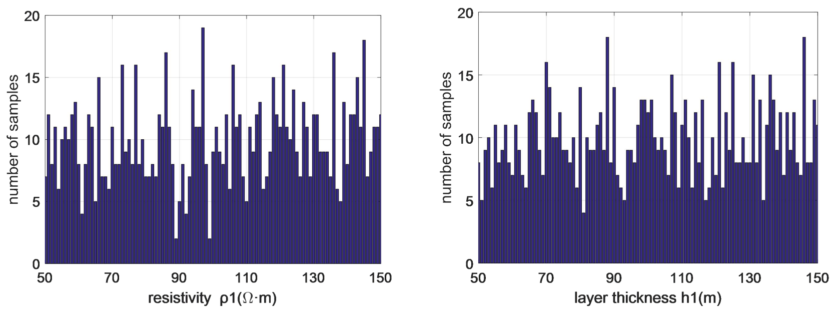

Fig. 6 Distribution of resistivity ρ_1 and thickness h_1 in training samples

The inversion results were shown in Table.4. and Fig.7~8. The BP type algorithms were superior to the NPGA inversion in Table.4. Moreover, the inversion accuracy, convergence rate and optimization ability of the COPSO-BP algorithm were better than others.

Table.4 Inversion comparison of three-layer H type geoelectric model

H type	resistivity ρ (Ω·m)			thickness h(m)		total relative error(%)
	ρ_1	ρ_2	ρ_3	h_1	h_2	
reference value	100	10	100	100	200	--
BP relative error(%)	-0.275	-0.625	0.765	-0.968	-0.649	3.284
SPSO-BP relative error(%)	0.062	-0.322	-0.737	-0.579	-0.970	2.672
COPSO-BP	100.031	9.991	99.310	100.234	200.886	--
COPSO-BP relative error(%)	0.031	-0.087	-0.689	0.234	0.443	1.487
NPGA relative error(%)	0.133	-0.034	3.450	-7.305	-0.401	11.323

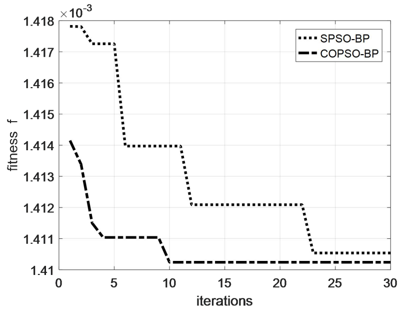

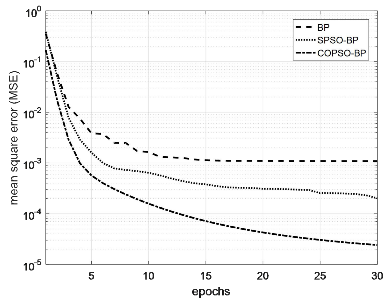

Fig. 7 Fitness curves of SPSO-BP and COPSO-BP **Fig. 8** Mean square error curves comparison

Additional results showed that the solution range of ρ_1 and h_1 in 20 times simulations for above algorithms were $\rho_1 \in (97.980, 103.102)$, $h_1 \in (96.962, 102.480)$ for BP, $\rho_1 \in (98.954, 101.137)$, $h_1 \in (96.955, 101.829)$ for SPSO-BP, $\rho_1 \in (99.382, 100.989)$, $h_1 \in (97.877, 101.044)$ for COPSO-BP respectively. Therefore, the COPSO-BP can acquire higher accuracy and is more stable.

(2) *5-layered KHK type model*

A 5-layered KHK type geoelectric model was adopted and its resistivity were $\rho_1 = 100$ Ω·m, $\rho_2 = 300$ Ω·m, $\rho_3 = 50$ Ω·m, $\rho_4 = 200$ Ω·m, $\rho_5 = 30$ Ω·m and thickness were $h_1 = 100$ m, $h_2 = 200$ m, $h_3 = 300$ m, $h_4 = 500$ m.

The training samples with parameter ranges were $\rho_1 \in (50,150)$, $\rho_2 \in (150,450)$, $\rho_3 \in (25,75)$, $\rho_4 \in (100,300)$, $\rho_5 \in (15,45)$ for resistivity, and $h_1 \in (50,150)$, $h_2 \in (100,300)$, $h_3 \in (150,450)$, $h_4 \in (250,750)$ for thickness. The 1000 groups training samples were generated within above ranges. The inversion results were shown in Table.5 and Fig.9~10. As can be seen that the COPSO-BP algorithm has better global optimization performance.

Table.5 Inversion comparison for five-layer KHK type geoelectric model

KHK type	resistivity ρ(Ω·m)					thickness h(m)				Total relative error(%)
	ρ_1	ρ_2	ρ_3	ρ_4	ρ_5	h_1	h_2	h_3	h_4	
reference value	100	300	50	200	30	100	200	300	500	--
BP relative error(%)	-1.006	-0.862	-1.014	-0.030	1.119	-0.362	-0.298	-0.575	-0.376	5.645
SPSO-BP relative error(%)	0.429	1.040	-0.577	-0.071	-0.883	-0.002	0.657	-0.655	-0.316	4.634
COPSO-BP	99.594	299.469	50.082	199.092	29.937	99.501	200.481	301.800	497.670	--
COPSO-BP relative error(%)	-0.405	-0.176	0.164	-0.453	-0.209	-0.498	0.240	0.600	-0.465	3.214
NPGA relative error(%)	-6.211	-0.008	-0.974	3.930	3.083	-0.691	0.505	-2.900	-3.370	19.062

https://doi.org/10.5194/npg-2019-36
Preprint. Discussion started: 2 July 2019

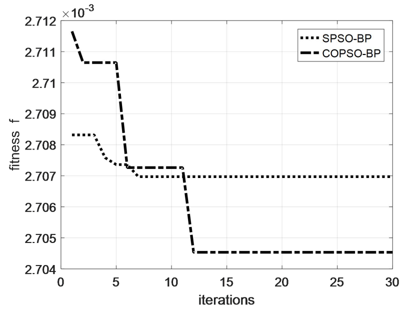

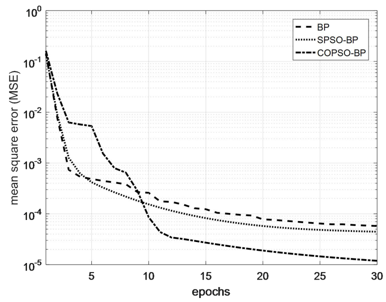

Fig. 9 Fitness curves of SPSO-BP and COPSO-BP **Fig. 10** Mean square error curves comparison

(3) ***Inversion comparison***

Three kinds of BP methods as traditional BP, the SPSO-BP and the COPSO-BP algorithms were compared in Table.6. Hence, the training times of COPSO-BP was obviously less than SPSO-BP and was almost equal to BP, it can obtain better precision especially for its global optimization performance.

Table.6 Simulation comparison for different algorithms

inversion method	three-layer H type model			five-layer KHK type model		
	training times	minimum training error	test relative error rate(%)	training times	minimum training error	test relative error rate(%)
BP	3	0.2882	3.284	5	0.3013	5.645
SPSO-BP	7	0.2832	2.672	15	0.2992	4.634
COPSO-BP	5	0.2725	1.487	6	0.2900	3.214

The inversion of COPSO-BP and NGPA were compared in Fig.11. The fitting ability of COPSO-BP was much better than NPGA.

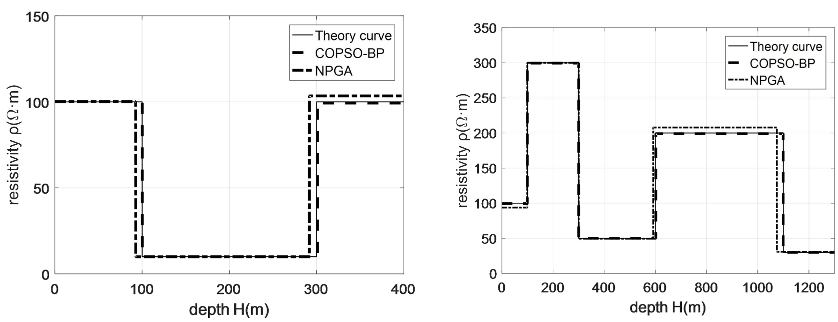

(a) Three-layer H type geoelectric model **(b)** Five-layer KHK type geoelectric model

Fig. 11 Inversion comparison for different geoelectric models

5 Conclusion

The nonlinear COPSO-BP method was proposed for TEM inversion. The BP's initial weight and

Nonlinear Processes in Geophysics
Discussions

threshold parameters were trained by COPSO algorithm which makes it not easy to fall into local optimum. The chaotic oscillation inertia weight for PSO was proposed so as to improve the PSO's global optimization ability and fast convergence in early stage. The layered geoelectric model inversion showed that the COPSO-BP method has better accuracy, stability and relative less training times.

Author Contributions

Huaiqing Zhang conceived this manuscript. Huaiqing Zhang and Ruiyou Li developed the main algorithmic idea and mathematical part. Ruiheng Li and Nian Yu carried out the simulation and data analysis. Qiong Zhuang completed the writing and interpretation of this manuscript. All authors contributed to the manuscript writing and approved the final manuscript.

Competing interests

The authors declare that they have no conflict of interest.

Acknowledgments

This work was partly supported by the National Natural Science Foundation of China (No.51377174, No.51577016, No.51877014), the Fundamental Research Funds for the Central Universities(No.2018CDQYDQ0005).

Computer Code Availability

Code name is PSOBP, developer is Huaiqing Zhang and Ruiyou Li, contact address is Chongqing University in China, telephone number is 13752954568 and e-mail is zhanghuaiqing@cqu.edu.cn, year first available, hardware required is a computer, software required is MATLAB R2016a, program language is C++, program size is 10KB, and source code from *https://github.com/liruiyou/PSOBP.*

Reference

Dai, Q., Jiang, F., and Dong, L.: Nonlinear inversion for electrical resistivity tomography based on chaotic DE-BP algorithm, J. Cent. South. Univ., 21, 2018-2025, https://doi.org/10.1007/s11771-014-2151-9, 2014.

Fernández Martínez, J. L., García Gonzalo, E., Fernández Álvarez, J. P., Kuzma, H. A., and Menéndez Pérez, C. O.: PSO: A powerful algorithm to solve geophysical inverse problems: Application to a 1D-DC resistivity case, Journal of Applied Geophysics, 71, 13-25, https://doi.org/10.1016/j.jappgeo.2010.02.001, 2010.

Godio, A., and Santilano, A.: On the optimization of electromagnetic geophysical data: Application of the PSO algorithm, Journal of Applied Geophysics, 148, 163-174, https://doi.org/10.1016/j.jappgeo.2017.11.016, 2018.

Wang, H., Liu M. L., Xi, Z. Z., Peng, X. L., He, H.: Magnetotelluric inversion based on BP neural network optimized by genetic algorithm, Chinese Journal of Geophysics, 61, 1563-1575 https://doi.org/10.6038/cjg

2018L0064, 2018.

Jha, M. K., Kumar, S., and Chowdhury, A.: Vertical electrical sounding survey and resistivity inversion using genetic algorithm optimization technique, J. Hydrol., 359, 71-87, https://doi.org/10.1016/j.jhydrol.2008.06.018, 2008.

Jiang, F., Dai, Q., and Dong, L.: An ICPSO-RBFNN nonlinear inversion for electrical resistivity imaging, J. Cent. South. Univ., 23, 2129-2138, https://doi.org/10.1007/s11771-016-3269-8, 2016a.

Jiang, F., Dai, Q., and Dong, L.: Nonlinear inversion of electrical resistivity imaging using pruning Bayesian neural networks, Journal of Applied Geophysics, 13, 267-278, https://doi.org/10.1007/s11770-016-0561-1, 2016b.

Jiang, F., Dong, L., and Dai, Q.: Electrical resistivity imaging inversion: An ISFLA trained kernel principal component wavelet neural network approach, Neural. Networks., 104, 114-123, https://doi.org/10.1016/j.neunet.2018.04.012, 2018.

Kaufman, A. A., and Keller, G. V.: Frequency and Transient Sounding, Elsevier Methods in Geochemistry & Geophysics, 1983.

Johnson, O. L., Aizebeokhai, A. P.: Application of Artificial Neural Network for the Inversion of Electrical Resistivity Data, Journal of Informatics and Mathematical Sciences, 9, 297-316, 2017.

Li, F. P., Yang, H. Y., and Liu, X. H.: Nonlinear programming genetic algorithm in transient electromagnetic inversion, Geophysical and Geochemical Exploration, 41, 347-353, 2017.

Maiti, S., Erram, V. C., Gupta, G., and Tiwari, R. K.: ANN based inversion of DC resistivity data for groundwater exploration in hard rock terrain of western Maharashtra (India), J. Hydrol., 464, 294-308, https://doi.org/10.1016/j.jhydrol.2012.07.020, 2012.

Pekşen, E., Yas, T., and Kıyak, A.: 1-D DC Resistivity Modeling and Interpretation in Anisotropic Media Using Particle Swarm Optimization, Pure. Appl. Geophys., 171, 2371-2389, https://doi.org/10.1007/s00024-014-0802-2, 2014.

Raj, A. S., Srinivas, Y. , and Oliver, D. H.: A novel and generalized approach in the inversion of geoelectrical resistivity data using Artificial Neural Networks (ANN), J. Earth Syst. Scl., 123, 395-411, https://doi.org/10.1007/s12040-014-0402-7, 2014.

Rosas-Carbajal, M., Linde, N., Kalscheuer, T., and Vrugt, J. A.: Two-dimensional probabilistic inversion of plane-wave electromagnetic data: methodology, model constraints and joint inversion with electrical resistivity data, Geophys. J. Int., 196, 1508-1524, https://doi.org/10.1093/gji/ggt482, 2014.

Shi, F., Wang, X. C., and YUN L.: Matlab neural network case study, The Beijing University of Aeronautics & Astronautics Press, Beijing, 2010.

Sharma, S. P.: VFSARES—a very fast simulated annealing FORTRAN program for interpretation of 1-D DC resistivity sounding data from various electrode arrays, Comput. Geosci., 42, 177-188, https://doi.org/10.1016/j.cageo.2011.08.029, 2012.

Srinivas, Y., Raj, A. S., Oliver, D. H., Muthuraj, D., and Chandrasekar, N.: A robust behavior of Feed Forward Back propagation algorithm of Artificial Neural Networks in the application of vertical electrical sounding data

Nonlinear Processes in Geophysics
Discussions

inversion, Geosci. Front., 3, 729-736, https://doi.org/10.1016/j.gsf.2012.02.003, 2012.

Tran, K. T., and Hiltunen, D. R.: Two-Dimensional Inversion of Full Waveforms Using Simulated Annealing, J. Geotech. Geoenviron. Eng., 138, https://doi.org/1075-1090, 2012.

Li, Y. Y., Chen, B. C., Zhao, Y. G., Yun, C., Ma, X. B., and Kong, X. R.: Nonlinear inversion for electrical resistivity tomography, Chinese Journal of Geophysics, 52, 758-764, https://doi.org/10.1016/S1003-6326(09)60084-4, 2009.

Zhang, L. Y., and Liu, H. F.: The application of ABP method in high-density resistivity method inversion, Chinese Journal of Geophysics., 54, 64-71, https://doi.org/10.1002/cjg2.1587, 2011.